Engineering Solid Mechanics 6 (2018) 307-314

Contents lists available at GrowingScience

Engineering Solid Mechanics

homepage: www.GrowingScience.com/esm

Numerical analysis of dynamic non-linear behavior of orthotropic multilayer shells with reinforcements in spirals

Emmanuel E.T. Olodo[a*], Olivier A. Passoli[a], Villevo Adanhounme[b] and Svetlana L. Shambina[c]

[a]*Laboratory of Applied Mechanics and Energetic (LEMA), University of Abomey-Calavi, Benin*
[b]*International Chair in Mathematical Physics and Applications (icmpa-Unesco Chair), University of Abomey-Calavi, Benin*
[c]*Engineering Faculty, Peoples Friendship University of Russia, Moscow, Russia*

A R T I C L E I N F O

Article history:
Received 10 June, 2018
Accepted 26 August 2018
Available online
26 August 2018

Keywords:
Wilkins algorithm
Orthogonal reinforcements
Symmetric reinforcements
Winding angle

A B S T R A C T

In the present work, an elasto-plastic model is proposed for the numerical analysis of dynamic nonlinear behavior of composite thick shells with reinforcements in spirals subjected to impulsive loading. Wilkins algorithm was taken to analysis physical and geometrical non-linearity of stress-strain state of elasto-plastic thick composite shells. This study is carried out on two types of cylindrical composite shells in different reinforcement winding angles and different magnitudes of impulse loads. By a calculation code in finite difference, first the influence of physical non linearity on the stress-strain state of cylindrical monolayer shell was established and then the relationship between residual strains and the winding angle of the symmetric reinforcements was investigated. Finally, the influence of the winding angle of the orthogonal reinforcements on the residual strains of a bilayer composite shell was analyzed numerically.

1. Introduction

The problem of the dynamics of composite membranes is undergoing a revival of interest in the scientific community because the areas of application more varied in the industrial sector including civil engineering. These structures are often subject to non-stationary solicitations, for example, the basic walls designed to keep their bearing capacity in extreme cases of sudden increase in work load. Today are widely used multilayer composite shells of revolution with reinforcements in spiral under angle α to the generatrix. Generally, such shells are locally orthotropic, however their main anisotropy axes x', φ', r in this case no coincide with axes of global system of cylindrical coordinates x, φ, r. Many works are carried out on such structure behavior in static regime (Li, 2007; Arashmehr et al., 2013; Rahimi et al., 2013). Same, composite shells explosion tests-related experimental data are available in technical literature (Fedorenko et al., 2005; Batra & Hassan, 2007; Leblanc & Shukla, 2010). Exact solutions to dynamic problems of composite cylindrical shells are mathematically involved and, in many cases, not available. Hence, most of available solutions are based on approximate methods. For the study of the dynamic behavior of composite shells, various numerical approaches are increasingly used. Thus finite element approaches are widely used to simulate the behavior of cylindrical shells under dynamic loading (Wang & Chen, 2004; Haldar, 2008; Perotti et al., 2013; Srinivasa et al., 2014). Interesting results are obtained by (Haftchenari et al., 2007; Alibeigloo, 2009) for the dynamic analysis

* Corresponding author.
E-mail addresses: olodoe@live.fr (E. E.T. Olodo)

doi: 10.5267/j.esm.2018.9.001

of composite cylindrical shells using differential quadrature method. Chakrabarti (2013) studied the dynamic response of a functionally graded shell using finite element formulation. Numerical results were presented for cylindrical and spherical shells for different boundary conditions. On the other hand, a number of studies based on Wilkins algorithm have been carried out for the numerical analysis of dynamic behavior of elastic multilayer cylindrical shells (Lugovoi et al., 2006; Rybakin et al., 2009). But most of the work on the study of these structures is carried out in small deformations. The studies in dynamics of the influence of the reinforcements in spirals on the stress-strain state of multilayer elasto-plastic shells (in the case of large deformations) are not available in the technical literature.

The purpose of this work is to propose a model based on Wilkins algorithm (Wilkins, 1964) in case of axisymmetric dynamic loading of multilayer orthotropic shells, taking into account geometrical and physical non-linearity, then to analyze the influence of various reinforcement schemes and types of non-linearity on the stress-strain state of thick-walled cylindrical shells subjected to axisymmetric impulsive action.

2. Material and methods

For mathematical formulation of the problem, we consider origin of coordinates in cylinder symmetry center. Governing motion equations in cylindrical coordinates, taking into account the axial symmetry and arbitrary reinforcement angle α (from 0 to 90 °) have form below:

$$\begin{aligned} &\frac{\partial \sigma_r}{\partial r} + \frac{\partial \tau_{rx}}{\partial x} + \frac{\sigma_r - \sigma_\varphi}{r} = \rho \frac{d u_r}{d t}, \\ &\frac{\partial \tau_{rx}}{\partial r} + \frac{\partial \sigma_x}{\partial x} + \frac{\tau_{rx}}{r} = \rho \frac{d u_x}{d t}, \\ &\frac{\partial \tau_{r\varphi}}{\partial r} + \frac{\partial \tau_{x\varphi}}{\partial x} + \frac{2\tau_{r\varphi}}{r} = \rho \frac{d u_\varphi}{d t}, \end{aligned} \tag{1}$$

where: ρ - The material density, $\sigma_r, \sigma_\varphi, \sigma_x, \tau_{rx}, \tau_{r\varphi}, \tau_{x\varphi}$ - components of stress tensor; t-time ; u_r, u_φ, u_x - components of displacement velocity vector.

Geometric relations have below form:

$$\dot{\varepsilon}_r = \frac{\partial u_r}{\partial r},\ \dot{\varepsilon}_\varphi = \frac{u_r}{r},\ \dot{\varepsilon}_x = \frac{\partial u_x}{\partial x},\ \dot{\gamma}_{rx} = \frac{\partial u_r}{\partial x} + \frac{\partial u_x}{\partial r},\ \dot{\gamma}_{r\varphi} = \frac{\partial u_\varphi}{\partial r} - \frac{u_\varphi}{r},\ \dot{\gamma}_{x\varphi} = \frac{\partial u_\varphi}{\partial x}. \tag{2}$$

Physical equations taking into account the reinforcement angle α (from 0 to 90 °) write in vector form:

$$\frac{d}{dt}\left\{\sigma_x, \sigma_\varphi, \sigma_r, \tau_{x\varphi}, \tau_{\varphi r}, \tau_{rx}\right\} = C\left\{\dot{\varepsilon}_x, \dot{\varepsilon}_\varphi, \dot{\varepsilon}_r, \dot{\gamma}_{x\varphi}, \dot{\gamma}_{\varphi r}, \dot{\gamma}_{rx}\right\} \tag{3}$$

Square matrix C size 6 x 6 is symmetric ($C_{ij} = C_{ji}$) and has following components:

$$C_{12} = B_{x\varphi} + \left(A_x + A_\varphi - 2B_{x\varphi} - 4G_{x\varphi}\right)\sin^2\alpha\cos^2\alpha,$$

$$C_{44} = G_{x\varphi}\cos^2 2\alpha + \left(A_x + A_\varphi - 2B_{x\varphi}\right)\sin^2\alpha\cos^2\alpha,$$

$$C_{33} = A_r,$$

$$\left\{C_{11}; C_{22}\right\} = \left\{A_x; A_\varphi\right\}\cos^4\alpha + \left\{A_\varphi; A_x\right\}\sin^4\alpha + \{1;1\}\left(0.5B_{x\varphi} + G_{x\varphi}\right)\sin^2 2\alpha,$$

$$\left\{C_{13}; C_{23}; C_{55}; C_{66}\right\} = \left\{B_{rx}; B_{\varphi r}; G_{\varphi r}; G_{rx}\right\}\cos^2\alpha + \left\{B_{\varphi r}; B_{rx}; G_{rx}; G_{\varphi r}\right\}\sin^2\alpha,$$

$$\left\{C_{34}; C_{56}\right\} = \left\{B_{\varphi r} - B_{rx}; G_{\varphi r} - G_{rx}\right\}\sin\alpha\cos\alpha,$$

$$\left\{C_{14}; C_{24}\right\} = \left[\left\{A_\varphi; -A_x\right\}\sin^2\alpha + \left\{-A_x; A_\varphi\right\}\cos^2\alpha + \{1;-1\}\left(B_{x\varphi} + 2G_{x\varphi}\right)\cos 2\alpha\right]\sin\alpha\cos\alpha,$$

$$A_x = E_x\left(1 - \upsilon_{\varphi r}\upsilon_{r\varphi}\right)/D_0,$$

$$B_{x\varphi} = E_\varphi\left(\upsilon_{x\varphi} + \upsilon_{xr}\upsilon_{r\varphi}\right)/D_0,$$

$$D_0 = 1 - 2\upsilon_{x\varphi}\upsilon_{\varphi r}\upsilon_{rx} - \upsilon_{x\varphi}\upsilon_{\varphi x} - \upsilon_{\varphi r}\upsilon_{r\varphi} - \upsilon_{rx}\upsilon_{xr},$$

Expressions of $A_\varphi, A_r, B_{\varphi r}, B_{rx}$ are obtained by cyclic permutation of indices x, φ, r.
$E_i, \upsilon_{ij}, G_{ij}$ ($i, j = x, \varphi, r;\ i \neq j$) are elastic constants of the orthotropic material to the main anisotropy axes for the angle α = 0 in case of the orthotropic cylindrical shell. The following conditions must be met:

$$E_i \upsilon_{ji} = E_j \upsilon_{ij}, \quad i \neq j. \tag{4}$$

For the studied materials, $D_0>0$. Considering that the studied materials have plastic properties, taking into account plastic deformations will be described by Mises-Hill theory of plastic flow for orthotropic materials without hardening (Hill, 1998). In this case, following the main anisotropy axes *x ', φ', r*, plasticity criterion will be written as follow:

$$2f = V(\sigma_{x'} - \sigma_{\varphi'})^2 + F(\sigma_{\varphi'} - \sigma_r)^2 + D(\sigma_r - \sigma_{x'})^2 + N\tau^2_{x'\varphi'} + V\tau^2_{\varphi' r} + M\tau^2_{rx'} \le 2, \tag{5}$$

where

$$\begin{aligned} V &= \sigma_{Tx'}^{-2} + \sigma_{T\varphi'}^{-2} - \sigma_{Tr}^{-2}, \\ F &= \sigma_{T\varphi'}^{-2} + \sigma_{Tr}^{-2} - \sigma_{Tx'}^{-2}, \\ D &= \sigma_{Tr}^{-2} + \sigma_{Tx'}^{-2} - \sigma_{T\varphi'}^{-2}, \\ N &= 2\tau_{Tx'\varphi'}^{-2}, \quad L = 2\tau_{T\varphi' r}^{-2}, \quad M = 2\tau_{Trx'}^{-2}, \end{aligned} \tag{6}$$

where σ_{Ti}, τ_{Tij} - the flow limits of orthotropic material according to corresponding main anisotropy axes. Plastic deformations can be written in following form:

$$\begin{aligned} d\varepsilon^p_{x'} &= d\lambda[V(\sigma_{x'} - \sigma_{\varphi'}) + D(\sigma_{x'} - \sigma_r)], \\ d\varepsilon^p_{\varphi'} &= d\lambda[F(\sigma_{\varphi'} - \sigma_r) + V(\sigma_{\varphi'} - \sigma_{x'})], \\ d\varepsilon^p_r &= d\lambda[D(\sigma_r - \sigma_{x'}) + F(\sigma_r - \sigma_{\varphi'})], \\ d\gamma^p_{x'\varphi'} &= d\lambda N\tau_{x'\varphi'}, \quad d\gamma^p_{\varphi' r} = d\lambda L\tau_{\varphi' r}, \\ d\gamma^p_{rx'} &= d\lambda M\tau_{rx'}, \end{aligned} \tag{7}$$

where

$$d\lambda = \left\{ V(Fd\varepsilon^p_{x'} - Dd\varepsilon^p_{\varphi'})^2 + F(Dd\varepsilon^p_{\varphi'} - Vd\varepsilon^p_r)^2 + D(Vd\varepsilon^p_r - Fd\varepsilon^p_{x'})^2 + (VF + \right. \\ \left. + DV + FD)^2 \left[\frac{(d\gamma^p_{x'\varphi'})^2}{N} + \frac{(d\gamma^p_{\varphi' r})^2}{L} + \frac{(d\gamma^p_{rx'})^2}{M} \right] \right\}^{\frac{1}{2}} \Big/ [\sqrt{2}(VF + DV + FD)] \tag{8}$$

For isotropic material we have:

$$V = F = D = N/6 = L/6 = M/6 = 1/\sigma_T^2 \tag{9}$$

The total strains are supposed to be the sum of the elastic and plastic deformations. Elastic components are determined by physical Eqs. (3) and plastic deformations are determined by Eqs. (5-8). These equations are added to the initial conditions and boundary conditions. The initial conditions are null and the boundary conditions are in forces or in displacements. On the other hand despite the presence of all components of displacement, stresses and deformations, boundary problem (1)-(8) will be axisymmetric insofar as none of its variables depends on angular coordinate φ. On basis of Eqs. (1-8), a program has been developed in finite difference for the numerical analysis of geometrical and physical non-linearity of the stress-strain state of multi-layer elasto-plastic cylinders with arbitrary reinforcement angle α of each layer.

3. Results and discussion

3.1 Simulation taking into account geometrical non- linearity

Object of this study material is a monolayer elastic composite shell T300/5208 with epoxy matrix, which elastic characteristics are the following (Onkar et al., 2007; Zhao & Cho, 2007) as illustrated in Table 1 and Table 2.

Table 1. Elastic characteristics of composite T300/5208

E_x, MPa	$1.325 \cdot 10^5$
$E_\varphi = E_r, MPa$	$1.08 \cdot 10^4$
$G_{\varphi r}$, MPa	3400
$G_{x\varphi}$,=G_{rx} , MPa	5700
$\upsilon_{x\varphi}$	0.24
$\upsilon_{\varphi r}$	0.49
υ_{rx}	0.02
ρ, kg/m^3	1540
α, rad	$\pi/3$

Table 2. Cylinder geometrical dimensions

Length, m	Internal radius, m	External radius, m
0.4	0.1	0.12

Material is loaded by internal axisymmetric impulsive pressure according to the following law (Baum et al., 1975):

$$\sigma_{r_{|r=R_1}} = -\sigma_0 R_1^3 l^{-3} H(la^{-1} - t), \tag{10}$$

where, a*=6310 m/s,* $l = \sqrt{x^2 + R_1^2}$ and H is Heaviside function.

Variation of the impulse amplitude is as follows:

1. $\sigma_0 = 1$ MPa - corresponding to linear behavior
2. $\sigma_0 = 1500$ MPa - corresponding to geometrically non-linear behavior

Ends and cylinder surface are free of any load. The simulation results are given by curves in Fig. 1.

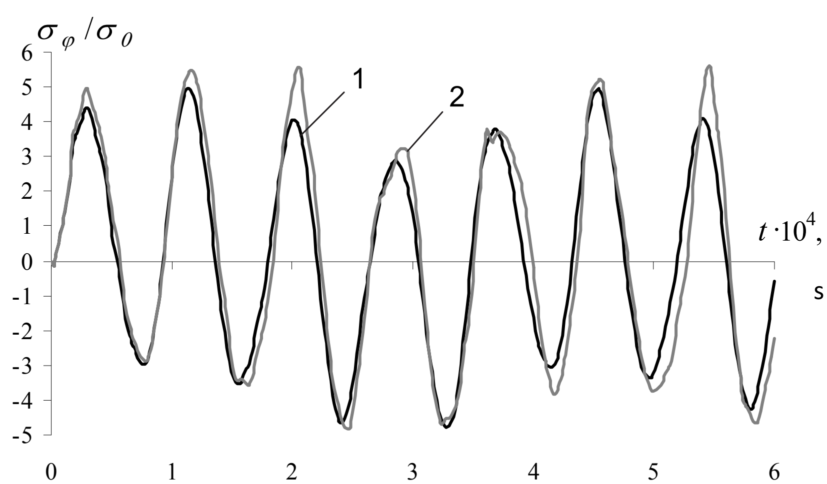

Fig. 1. Influence of the geometrical nonlinearity on the circular stresses in the mono-layer composite shell

Curve 1 corresponds to linear behavior (σ_0 =1MPa, where maximum deformations do not exceed 0.008%), curve 2 corresponds to geometrically non-linear behavior (σ_0 = 1500 MPa where maximum deformations can reach 15%). As seen in Fig. 1 the curves 1 and 2 are similar. Torsional vibration and transverse vibration are linked by longitudinal vibration mode and occur with the same frequency. Radial vibration corresponds to another vibration mode and occurs with greater frequency. Studied shell being short cylindrical shell subjected to axisymmetric internal pressure, cannot hardly expect large rotations even in presence of intensive load. Rotations will be still less significant compared with corresponding deformations. Therefore, the effects related to the consideration of geometrical nonlinearity of such structures are relatively moderate: qualitatively these effects have little influence on dynamic impulse mapping, but quantitatively they produce important values of the amplitudes of kinematic parameters and forces compared to the linear approach.

3.2. Simulation taking into account physical non-linearity

3.2.1 Single-layer cylindrical shell

We study the same previous composite shell but with elasto-plastic behavior. Resistance limits of epoxy composite T300/5208 are given by (Onkar et al., 2007). Whereas most composites have relatively low plastic zones on the corresponding deformation curves, using data from (Onkar et al., 2007), we will adopt following values of the flow limits for composite T300/5208: σ_{Tx}=1500 MPa; $\sigma_{T\varphi}=\sigma_{Tr}$=40 MPa; $\tau_{T\varphi r}$=65 MPa; $\tau_{Tr\,x}=\tau_{Tx\varphi}$=85 MPa. Calculation results are presented in Figs. 2 and 3. In figure 2 the curve numbering match the different values of impulse magnitudes σ_0. Thus, for the curves 1, 2, 3, 4, 5, σ_0 values are 20MPa, 50MPa, 100MPa, 300MPa, 400MPa, respectively. The curves in figure 2 show influence of physical nonlinearity on the stress-strain state of the monolayer cylindrical shell. On the other hand, figure 2-e shows variation in time of the radial displacement in vicinity at end of the internal surface of cylindrical shell ($r = R_1$; $x=L/2$). For σ_0=20 MPa (curve 1), the shell undergoes elastic deformation while for $\sigma_0 \geq$50 MPa, it undergoes elasto-plastic deformation.

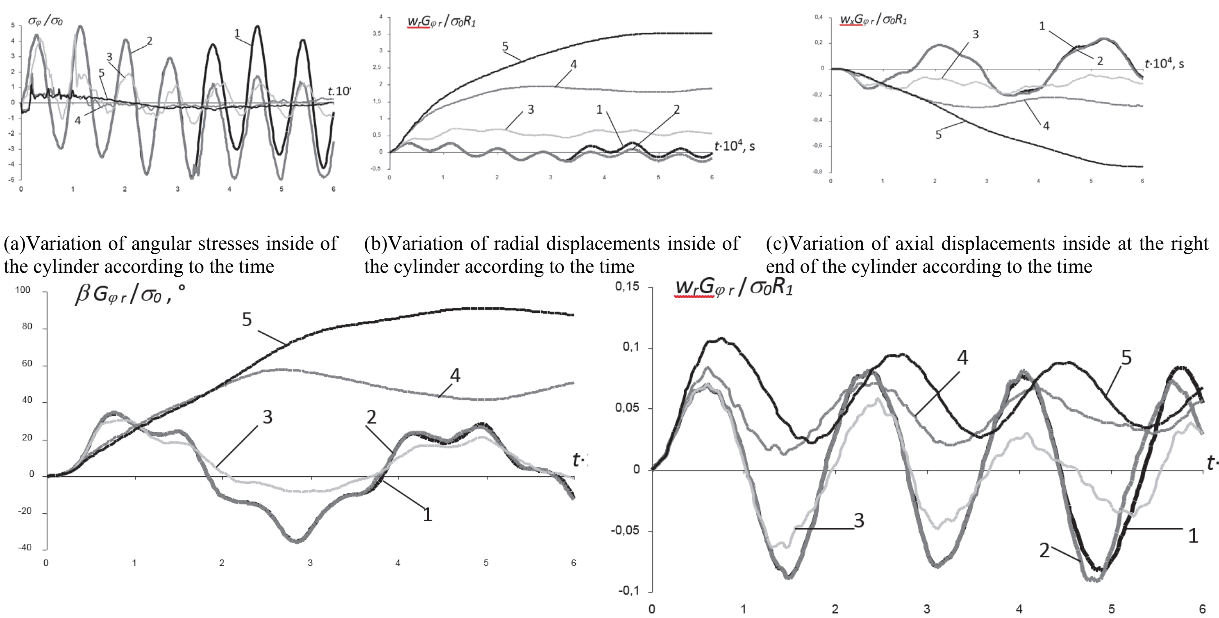

(a)Variation of angular stresses inside of the cylinder according to the time

(b)Variation of radial displacements inside of the cylinder according to the time

(c)Variation of axial displacements inside at the right end of the cylinder according to the time

(d) Variation of the torsional angle of the right end over the left end of the cylinder according to the time

(e) Variation of radial displacement inside at the right end of the cylinder according to the time

Fig. 2. Influence of physical nonlinearity on the stress-strain state of the monolayer cylindrical shell

The singularity is that for relatively moderate load (σ_0 =50 MPa), the plastic deformations do not occur immediately but rather by "pitch effect". At time $t_0 \approx 3{,}3 \cdot 10^{-4}$s the shell has perfectly elastic behavior, curves 1 and 2 coincide (by comparison, the action of impulsive load time is approximately$1{,}65 \cdot 10^{-5}$s thus 20 times smaller). When $t \geq t_0$ it begins with occur local plastic zones due to the ‘’pitch effect ‘', what is reflected by divergence of the curves 1 and 2. When $\sigma_0 \geq$100MPa the shell residual deflections, elongations and torsion angles will appear. For large loads these quantities leads to quasi-stationary values. In addition for σ_0=400 MPa one observe elastic vibrations around the residual deflection (Fig. 2-e, curve 5).

3.2.2 Bilayer cylindrical shell

Geometrical dimensions and loading are the same as previously. The two layers have the same thickness and the same composite material T300/5208. Reinforcement winding angle of each layer being different, two reinforcement schemes have been studied:

1. Symmetric reinforcement: in the internal layer, reinforcement winding angle is (+ ∝), in the external layer, reinforcement winding angle is (-α);
2. Orthogonal reinforcement: in the external layer, reinforcement winding angle is (+ ∝), in the internal layer, reinforcement winding angle is (∝±90 °).

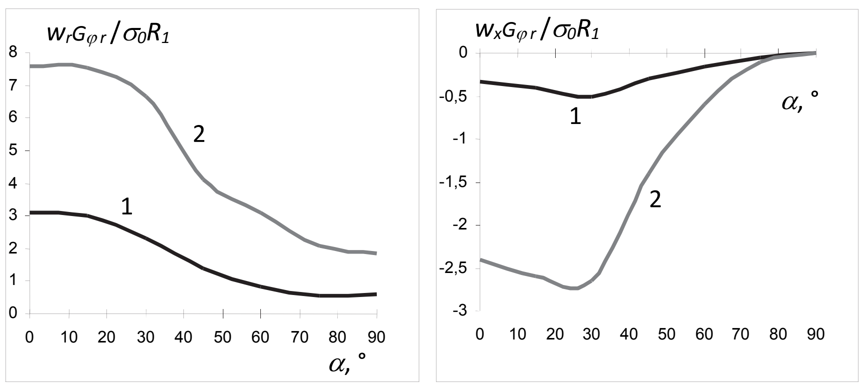

a) Radial displacements b) Axial displacements

Fig. 3. Residual deformation curves- function of symmetrical reinforcement winding angle α

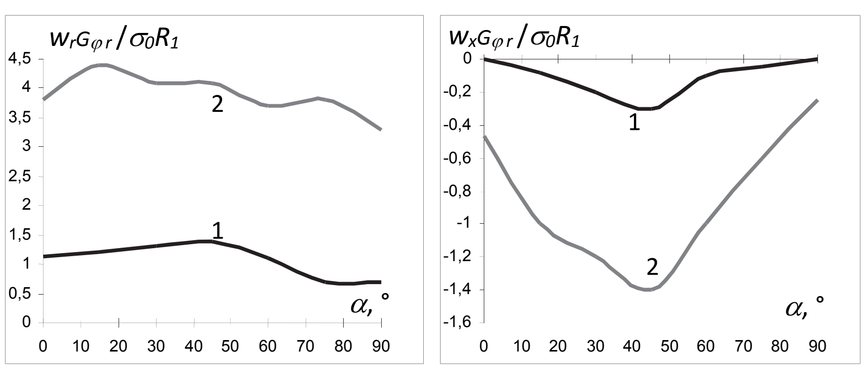

a) Radial displacements b) Axial displacements

Fig. 4. Residual deformation curves- function of orthogonal reinforcement winding angle ∝

Analysis also focuses on the relationship between the residual strains and reinforcement winding angle ∝. Calculation results are presented in Figs. 3 and 4 where curves 1 correspond to σ_0=200MPa while curves 2 correspond to σ_0=400MPa. There also observed strong nonlinear dependence between residual deformations, loading amplitude, winding angle and reinforcement scheme. Residual torsion for symmetric reinforcement is 10 times lower than orthogonal reinforcement. There is maximum residual deflection of central section with symmetric reinforcement. For the orthogonal reinforcement, this deflection is two- three times lower, depending on loading magnitude. The orthogonal reinforcement produces low level of residual elongation for winding angle α between 0 ° and 45 °. When α > 45 ° and σ_0=400MPa, there is low level of residual elongations with symmetrical reinforcements. Furthermore, the two schemes of reinforcement produce roughly the same values of residual radial deformations, qualitatively $\varepsilon_r(\alpha)$ mapping depends greatly on reinforcement scheme and σ_0.We can see that taking into account plastic deformation of composite shells has a great influence both qualitative and quantitative on the dynamic and residual stress state relate to geometrically nonlinear effects. The stress state depends non-linearity on the load magnitude, elasticity and flow characteristics, winding angle and reinforcement scheme.

4. Conclusion

This work was the result of numerical study of the dynamic nonlinear behavior of two composite shells, a monolayer and other bilayer, subjected to dynamic impulse loading. On basis of Wilkins algorithm, it is conducted analysis of influence of physical and geometrical nonlinearity on stress-strain state of elasto-plastic thick shells with different reinforcement schemes and different loading magnitudes. Obtained results have focused primarily on the following:

1. Analysis of influence of the geometrical nonlinearity on circular stresses of cylindrical mono layer composite shell
2. Analysis of influence of physical nonlinearity on the stress-strain state of mono layer composite shell taking into account the plastic deformations
3. For bilayer cylindrical shell, it is shown the relationship between the residual plastic deformation and the symmetrical reinforcement winding angle α
4. For this same bilayer composite shell it is shown the dependence between the residual plastic deformation and the orthogonal reinforcement winding angle α.

References

Alibeigloo, A. (2009). Static and vibration analysis of axi-symmetric angle-ply laminated cylindrical shell using state space differential quadrature method. *International Journal of Pressure Vessels and Piping*, *86*(11), 738-747.

Arashmehr, J., Rahimi, G. H., & Rasouli, S. F. (2013). An experimental and numerical investigation of a grid composite cylindrical shell subjected to transverse loading. *Strojniški vestnik-Journal of Mechanical Engineering*, *59*(12), 755-762.

Batra, R. C., & Hassan, N. M. (2007). Response of fiber reinforced composites to underwater explosive loads. *Composites Part B: Engineering*, *38*(4), 448-468.

Baum, F.A., Orlenko, L.P. and Stanyukovich, K.P. (1975). Physics of Explosion. Moscow: Nauka, (In Russian).

Fedorenko, A. G., Syrunin, M. A., & Ivanov, A. G. (2005). Criterion for selecting composite materials for explosion containment structures. *Combustion, Explosion and Shock Waves*, *41*(5), 487-495.

Chakrabarti, A. (2013). Dynamic response of functionally graded skew shell panel. *Latin American Journal of Solids and Structures*, *10*(6), 1243-1266.

Haftchenari, H., Darvizeh, M., Darvizeh, A., Ansari, R., & Sharma, C. B. (2007). Dynamic analysis of composite cylindrical shells using differential quadrature method (DQM). *Composite Structures*, *78*(2), 292-298.

Haldar, S. (2008). Free vibration of composite skewed cylindrical shell panel by finite element method. *Journal of Sound and Vibration*, *311*(1-2), 9-19.
Hill, R. (1998). *The mathematical theory of plasticity* (Vol. 11). Oxford university press.
LeBlanc, J., & Shukla, A. (2010). Dynamic response and damage evolution in composite materials subjected to underwater explosive loading: an experimental and computational study. *Composite Structures*, *92*(10), 2421-2430.
Li, G. (2007). Experimental study of hybrid composite cylinders. *Composite Structures*, *78*(2), 170-181.
Lugovoi, P. Z., Meish, V. F., Rybakin, B. P., & Sekrieru, G. V. (2006). Dynamics of reinforced compound shells under nonstationary loads. *International Applied Mechanics*, *42*(4), 455-460.
Onkar, A. K., Upadhyay, C. S., & Yadav, D. (2007). Probabilistic failure of laminated composite plates using the stochastic finite element method. *Composite Structures*, *77*(1), 79-91.
Perotti, L. E., Deiterding, R., Inaba, K., Shepherd, J., & Ortiz, M. (2013). Elastic response of water-filled fiber composite tubes under shock wave loading. *International Journal of Solids and Structures*, *50*(3-4), 473-486.
Rahimi, G. H., Zandi, M., & Rasouli, S. F. (2013). Analysis of the effect of stiffener profile on buckling strength in composite isogrid stiffened shell under axial loading. *Aerospace science and technology*, *24*(1), 198-203.
Rybakin, B., G. Secrieru, G., Lugovoi, P. & Meish, V. (2009). The numerical investigation of reinforced shell undergo dynamic load. SISOM 2009, Bucharest.
Srinivasa, C. V., Suresh, Y. J., & Kumar, W. P. (2014). Experimental and finite element studies on free vibration of skew plates. *International Journal of Advanced Structural Engineering (IJASE)*, *6*(1), 48.
Wang, H. J., & Chen, L. W. (2004). Finite element dynamic analysis of orthotropic cylindrical shells with a constrained damping layer. *Finite Elements in Analysis and Design*, *40*(7), 737-755.
Wilkins, M. L. (1964). Calculation of elastoplastic flow. Methods in Computational Physics, New York, Academic Press.
Zhao, G. P., & Cho, C. D. (2007). Damage initiation and propagation in composite shells subjected to impact. *Composite Structures*, *78*(1), 91-100.